Displays 36 (2015) 21–29

Contents lists available at ScienceDirect

Displays

journal homepage: www.elsevier.com/locate/displa

Developing novel liquid crystal technologies for display and photonic applications

Hari M. Atkuri [a], Eunice Sok Ping Leong [b], Jeoungyeon Hwang [c,d], Giovanna Palermo [e], Guangyuan Si [f], Jenny-Marie Wong [d], Liang-Chy Chien [d], Ji Ma [d], Kaichang Zhou [g], Yan Jun Liu [b], Luciano De Sio [c,e,*]

[a] R&D Engineer, Cardinal IG Technology Center, 7201 W Lake St, Minneapolis 55426, MN, USA
[b] Institute of Materials Research and Engineering, Agency for Science, Technology and Research (A*STAR), Singapore 117602, Singapore
[c] Beam Engineering for Advanced Measurements Co., Winter Park, FL 32789, USA
[d] Liquid Crystal Institute, Kent State University, Kent, OH 44240, USA
[e] Department of Physics and Centre of Excellence for the Study of Innovative Functional Materials (CEMIF-CAL), University of Calabria, Arcavacata di Rende 87036, Italy
[f] College of Information Science and Engineering, Northeastern University, Shenyang, Liaoning 110004, China
[g] First Solar Inc., Toledo, OH 43604, USA

ARTICLE INFO

Article history:
Received 19 August 2014
Received in revised form 8 October 2014
Accepted 24 October 2014
Available online 11 November 2014

Keywords:
Liquid crystals display
Nanoimprint lithography
Blue phase
Polymer
Electrofluidic

ABSTRACT

Modern liquid crystal displays (LCDs) require novel technologies, such as new alignment methods to eliminate alignment layers, fast response and long operation time. To this end, we report an overview of recent efforts in LCD technologies devoted to realize more display modes having no alignment layer, faster switching time and low battery consumption. In particular, we overview recent advances on the liquid crystals (LCs) alignment for display applications, which includes superfine nanostructures, polymeric microchannels and polymer stabilized LCs. Furthermore, we analyze the main optical and electro-optical properties of new generation LCDs displays addressing a particular attention to LCs blue phase hosting gold nanoparticles. Moreover, we focus on the progress of electrofluidic displays, which demonstrates characteristics that are similar to LCDs, with attention on various pixel designs, operation principles and possible future trends of the technology.

1. Advances in liquid crystal alignment for displays

Liquid crystal displays (LCDs) have become important and indispensable in our everyday life due to their compact size, low power consumption and high-resolution density. The portability and compactness of LCDs have initiated and driven new applications and markets such as notebooks, smartphones and large display video cameras [1–4]. All the achievements obtained in the LCDs field have been possible thanks to the decades of extensive research in liquid crystals (LCs) materials. Such extensive research has spearheaded a number of scientific and technical advances with day-to-day applications. LCs are a key component of the displays used in most laptop computers and the increasingly-popular flat panel televisions. Controlled by a network of transistors, LCs change their optical characteristics in response to electrical signals to create the text and images we see. Manufacture of the panels is complex, requiring multiple steps that can introduce defects. Among the steps is the application of a polymer film (e.g. rubbed polyimide (PI)) the so-called alignment layer to the two pieces of conductive glass between which the LCs operate. The film, which must be rubbed after being coated on the glass, anchors the LCs with a fixed alignment. The process of rubbing to create the necessary alignment can damage some of the transistors and introduce dust, producing defects that can reduce the manufacturing yield of the panels. To overcome these issues, various LC alignment techniques have been investigated as alternatives for the PI rubbing approach. Photo-alignment [5–7], ion beam bombardment [8,9], and oblique evaporation of silicon oxide (SiOx) film [10,11] are some of the potential approaches of LC alignment; however alignment instability, materials stability, non-smooth alignment, and low anchoring issues require consideration. Despite the availability of above-cited methods, the possibility of realizing a "surfactant free method" to align any kind of LC and self-organizing material is still an argument of ongoing research. In this section, we will focus on the recent advances on the LC alignment based on nanoimprint lithography (NIL) and an optical active polymeric template realized is soft-composite materials.

* Corresponding author at: Department of Physics and Centre of Excellence for the Study of Innovative Functional Materials (CEMIF-CAL), University of Calabria, Arcavacata di Rende 87036, Italy.
E-mail address: luciano.desio@fis.unical.it (L. De Sio).

http://dx.doi.org/10.1016/j.displa.2014.10.006
0141-9382/

1.1. LC alignment by means of NIL technique

Surface grooves with a suitable pitch and depth are effective in aligning LCs [12,13]. NIL can generate these grooves with a stable and precise pitch so as to lead to good LC alignment. Thus, NIL enables us to precisely control the direction of surface anisotropy and the surface anchoring strength through control of the pitch and depth on a mold, which is hardly possible in the conventional rubbing process. Fig. 1a shows a typical nanoimprinting process. A hard mold that contains the designed features is pressed into a polymeric layer on a substrate at a controlled temperature and pressure, thereby creating a thickness contrast in the polymeric material. A thin residual layer of polymeric material is inevitably left underneath the mold protrusions, and serves as a soft buffer layer that prevents damages of the hard mold on the substrate and effectively protects the delicate nanoscale features on the mold surface. After imprinting, the mold patterns are clearly imprinted into the film having the correspondence as the mirror image each other. This imprint process can be repeated across the substrate areas to obtain multiple imprint fields on the substrate. Fig. 1b and c shows top and cross-sectional scanning electron microscopy (SEM) images of an imprinted nanograting in polymethylmethacrylate (PMMA) [14]. The high-throughput, ultrahigh resolution, and low-cost fabrication makes NIL an attractive and widely researched technology for many applications, such as IC semiconductor device, nanophotonics, and displays. Most imprinting processes can be classified in two main categories: themo-printing and flash-printing, which require the imprinted materials be thermo-curable and photo-curable, respectively. NIL can enable periodic 1D, 2D and 3D structures [15–20], hence having the potential to align LCs in different ways. Various choice of imprinting materials will also affect the LC alignment. Poineer exploration work regarding the LC alignment on the imprinted surfaces has been done in the past decade [21–23]. For LC alignment, materials such as PMMA, poly(dimethylsiloxane) (PDMS), polyimide, SU-8 and polyurethane, have been widely tested. Among them, PMMA, one of common materials for the NIL, is used as a resist material because it has favorable thermal–mechanical properties. The low glass transition temperature (T_g): 90–100 °C, which is a favorable condition to avoid the damage of patterns on a mold surface. Depending on the imprinted material properties, both homogenous and homeotropic alignment can be achieved. For examples, Lin and Rogers have reported parallel LC alignment using three different alignment materials based on the same imprinting mold [24]. The three different materials are a photocurable polyurethane formulation (NOA 73, Norland Inc.), a thermally curable epoxy (SU-82, Microchem Corp.) and photocurable acrylate/methacrylate formulation (SK9, Summers Optical Inc.), respectively. All these three materials have excellent alignment capabilities once they are imprinted using a master PDMS mold. The LC alignment on the imprinted surfaces can be examined under the polarized optical microscope (POM). If the POM images show very uniform darkness and brightness, this indicates that the imprinted surface successfully aligns the LC molecules. In Ref. [25], researchers fabricated a vertically aligned cell using the nanopattern alignment layer. The nanopattern directions on both substrates were parallel to each other, and the cell gap was about 5 μm. Fig. 2 shows the POM view of the sample under the off and on states of the LC cell. In the off state, LC molecules remain perpendicular to the nanopattern surface and the light transmission is prohibited, resulting in a dark image (Fig. 2a). When an external electrical field is applied to the cell (on state), LC molecules shift to a horizontal position, parallel to the NP surface, and the NP LC cell clearly transmits visible light generated from backlight units, resulting in a white image (Fig. 2b). This indicates that uniform alignment was achieved for the NP LC cell. Investigation of the electro-optical properties is a direct way to examine the potential of a nanoimprint technique for LCD applications. Using the imprinted pattern as the alignment layer, a LC cell working in different modes can be assembled and assessed in terms of various parameters (threshold, response times, contrast, etc.) that indicate the performance of display devices. For example, Takahashi et al. have successfully demonstrated homogenous LC alignment using 50 nm ultrafine line and space nanogratings [26]. A twisted nematic (TN) LC cell using the nanogratings as alignment layers showed excellent electro-optical characteristics, as shown in Fig. 3. The measured contrast ratio of the TN cell was 44:1. NIL presents great opportunities for LC alignment. Despite their advantages over the conventional rubbing method, current NIL and platforms are in the infancy stage and require further improvements in various aspects for practical applications. In particular, it is still very challenging to achieve large-area and uniform imprinted pattern for LC

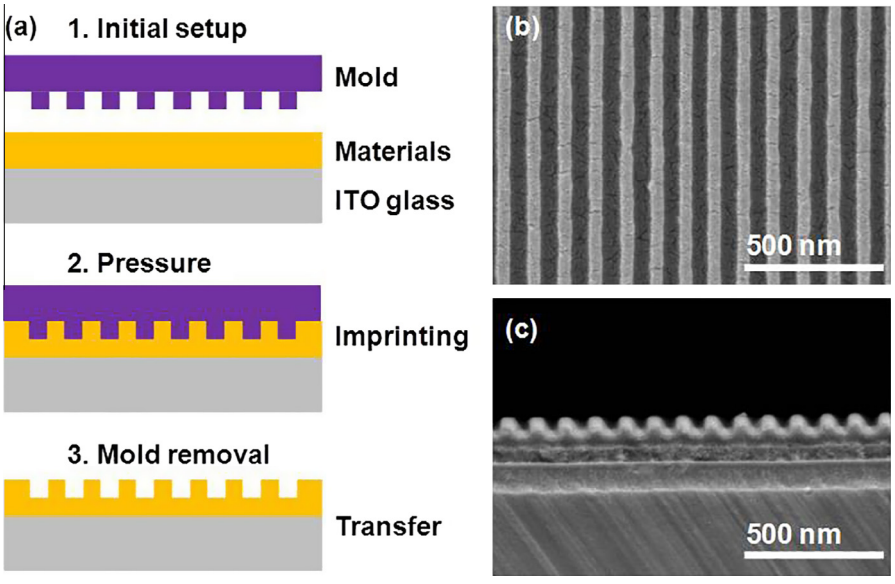

Fig. 1. Typical nanoimprinting process (a); SEM images of top (b) and cross-sectional (c) views of an imprinted nanograting. Figure (b) and (c) is adapted from Ref. [14].

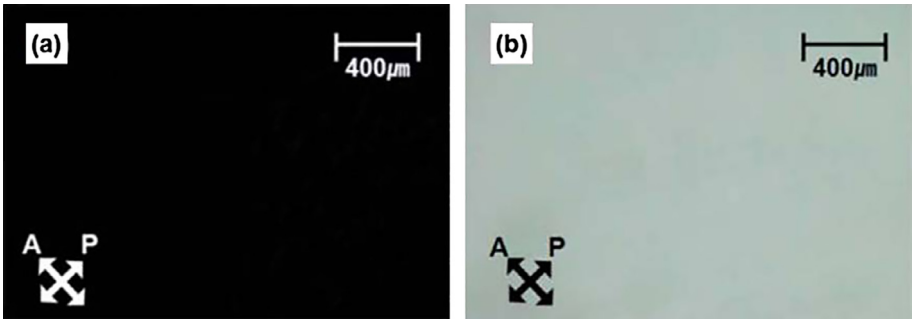

Fig. 2. Optical microscopic images of the homeotropic LC alignment under crossed Nicols: (a) off-state with no applied voltage and (b) on-state with applied voltage of 5 V. This figure is adapted from Ref. [25].

alignment. With increasing demand for nano/micro-patterns on large substrates, the establishment of large-scale fabrication technology for such patterns has become a priority. Continuous roller imprinting presents a low cost, high throughput solution without the size restrictions of batch mode imprinting. Currently the highest reported sustainable throughputs are 3 m/min for thermal roller imprinting [27] and 5 m/min for UV roller imprinting [28]. More recently, Guo and his coworkers have unveiled a newly completed six-inch roll-to-roll and roll-to-plate capable apparatus and demonstrated four-inch wide continuous imprinting of about 300 nm linewidth and 700 nm period gratings [29]. With the rapid development of the roller imprinting, it is therefore anticipated that over the coming years, fabrication of micro- and nano-scale structures over larger areas at a low cost will become industrially possible, hence making the large-area and uniform LC alignment feasible in developing novel LCDs.

1.2. LCs order in polymeric template

Few years ago Umeton and his coworkers [30] have realized a new kind of switchable diffraction grating named POLICRYPS (acronym of "alternation of POLymer–LIquid CRYstal–Polymer Slices"), which is made of slices of almost pure polymer, alternated to films of well aligned NLCs. This composite structure is obtained by irradiating a homogeneous syrup of NLC BL-001 and prepolymer (NOA-61 by Norland, containing a UV sensitive photoinitiator), 28% and 72% in weight respectively, with an interference pattern of UV light, under suitable experimental and geometrical conditions. The curing process is carried out at a 100 nm precision level, by utilizing an optical holographic setup that enables the spatial periodicity of the structure to be easily varied from the almost nanometric to the micrometric range [31]. Later on, it has been demonstrated that the POLICRYPS represents an excellent candidate to be used as a passive matrix for applications, due its unique morphological properties; in fact, the pure NLC confined between the polymeric slices can be easily removed in a selective way by exploiting a microfluidic etching process without opening the glass cell and the sample appears as made of sharp polymer slices separated by empty channels. Subsequently, the empty polymeric template (Fig. 4a) can backfilled with different materials including NLCs [32] cholesteric LCs (CLCs) [33], ferroelectric LCs (FLCs) [34], or liquid crystalline DNA [35] while imparting long-range macroscopic alignment. In order to show the extraordinary capability of the empty polymeric template to induce long range order in LCs compounds without any surface treatments, the empty POLICRYPS template (Fig. 4a) has been back filled with the same NLC used during the curing process. The sample was infiltrated with NLC BL-001 at elevated temperature (70 °C) during the filling process to ensure that a complete transition to the isotropic state ($T_{N–I}$ = 67 °C) had occurred. The self-organization process giving rise to uniform and stable alignment of the NLC within the micro-channels is induced after the filling process by slowly (0.5 deg/min) cooling down the sample to room temperature. The excellent optical quality of the sample is evident in the POM image of Fig. 4e and reflects the good NLC alignment. One more interesting aspect is represented by the possibility of realizing 2D composite photonic devices. First, the "empty POLICRYPS" structure has been infiltrated with the same curing mixture used for the fabrication of 1D POLICRYPS. A 2D grid is then obtained by simply rotating the sample and following again the standard two-beam interference procedure utilized for the POLICRYPS fabrication, without the need of any multiple beam interference pattern. The versatility of this technique allows choosing the geometry of the unit cell of the grid such as square hole geometry obtained with a 90° rotation before operating of the second curing step (Fig. 4b) and a "lozenge" hole geometry obtained by a 45° rotation utilized for the second curing step (Fig. 4c). Both geometries enable realization of microdomains with a strong asymmetry of the NLC director orientation as verified by POM analysis reported in Fig. 4f–g. The self-organization of LCs components on curved geometries represents also a very important key point for the realization of novel flexible displays. To this end, very recently De Sio et al. [36] have exploited the possibility to utilize the POLICRYPS technique for fabricating curved NLC geometries making use of a simplified (single beam curing process) holographic setup without the need for holographic mixing of two input beams. The gratings are photochemically formed using a single beam imaged through a commercially available Fresnel mask onto a glass cell which contains a slight modified curing mixture used for the fabrication of conventional POLICRYPS structures. The regular mixture composed by NLC BL-001 and NOA-61 was modified by adding a small amount (1% in weight) of the visible

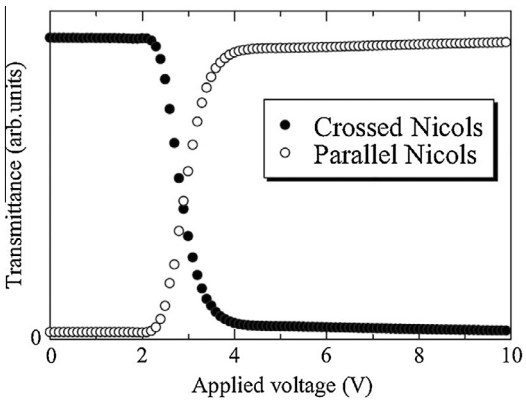

Fig. 3. Transmittance versus voltage characteristics of the nanogrooved LC cell. This figure is adapted from Ref. [26].

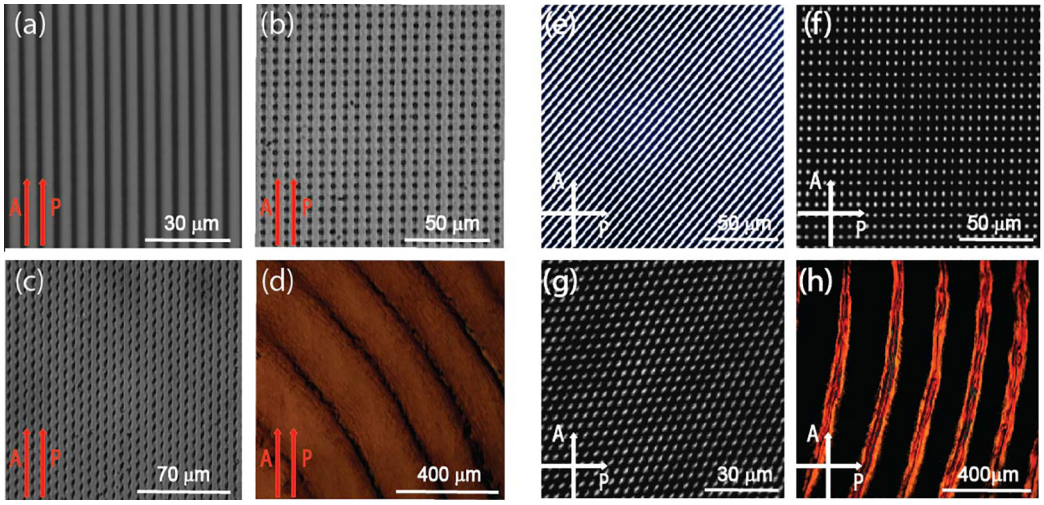

Fig. 4. POM view of the polymeric template (a, e), 2D polymeric grid (b, f), lozenge hole geometry (c, g) and curved polymeric walls (d, h) between parallel and crossed polarizers respectively.

photoinitiator (Irgacure 784) in order to reduce the attenuation of the glass substrates as they absorb in the UV range. Fig. 4d is a polarized image of a circular POLICRYPS structure, exhibits concentric rings with a varying inter-distance made of curved polymeric slices which alternates with channels of well aligned NLC whose the molecular director is radially aligned to the polymeric slices as is evident high magnification POM images reported in Fig. 4h. The technologies proposed here include not only absence of an alignment layer but also absence of haze, robust structure and inexpensive manufacturing. This is a unique opportunity and a big advantage compared to conventional liquid crystal devices. To date one of the main drawback of the standard two-beam interference procedure utilized for the POLICRYPS fabrication is represented by the impossibility to realize large area (more than 3 inches in diameter) structures. This technological limitation can be solved by patterning different POLICRYPS structures on the same substrate while minimizing the edge effect by means of a high precision level motor stage. However, it is worth pointing out that the actual POLICRYPS size (3 inches) is a "ready to go" technology for application such as smart-phones, digital watches and camera lenses.

2. LCs blue phase hosting gold nanoparticles for fast switching display

Cholesteric blue phase liquid crystals (BPLCs) are highly chiral materials that self-organize into an arrangement characterized by strong helical twisting along any radial direction around a central director that is perpendicular to all twist axes, which are the so-called double twisted cylinders [37]. Blue phases (BP) exist within a very narrow temperature range between the isotropic and cholesteric phases. A total of three types of blue phases, Blue phase (BP) I, BP II, and BP III, were discovered. Two (BP I and BP II) of the three types of blue phases pack into a cubic lattice on a scale ranging from one to two hundreds of nanometers, while the third type (BP III) is amorphous. The field-induced birefringence, the so-called Kerr effect, in a BPLC has been reported without the alignment layers. Recently, the polymerization of a small amount of reactive monomer in a BPLC has been another breakthrough. The phase-separated polymer tends to nucleate at the defect regions and is capable of stabilizing the cubic lattice against the temperature variation [38]. With the discovery of new BPLC mixtures and polymer composites, fast switching displays have been explored [39]; however, the issues of high switching voltage, hysteresis, light scattering and long-term stability are still challenges for practical applications. Here, we report study of the dispersion of gold nanorods (AuNR) in liquid crystal blue phase and investigate fundamental that may lead to the extended BP temperature range and enhanced electro-optical performance. A BPLC mixture was prepared using a nematic LC (55.0% of BL006, $\Delta n = 0.289$, $\Delta\varepsilon = +17.0$ purchased from Merck) and chiral dopant (45.0% of R811, HTP of 9.8 13.8 μm^{-1} purchased from Merck) to give a helical pitch around 160 nm. Lab-synthesized with organo thio-modified AuNR dispersed in dichloromethane (DCM) with size of 10 nm in diameter and 25–30 nm in length according to the information obtained from TEM study (Fig. 5a), was used as a nanoparticle additive. The doped BP LC mixtures were prepared by adding 0.6% of AuNR in the BP mixture, while keeping the nematic and chiral dopant at a constant 1: 0.8 ratio. A computer-controlled hot stage and a polarization microscope were used to determine the BP phase range. All samples were heated to the isotropic phase and cooled at a rate of 0.2 °C/min to room temperature. The reflection spectra were acquired with an Ocean Optics spectrometer as the temperature was varied.

Electro-optical (E-O) measurements of field induced birefringence required the use of in-plane-switching (IPS) cells with patterned indium tin oxide (ITO) of 5 μm electrode line and 5 μm electrode space on one glass substrate. The IPS cells were assembled with a second glass substrate, without ITO electrode, using ball spacers to separate the glass substrates with a cell gap of 5 μm (5/5/5). Through the use of capillary action the BP LC samples were filled at an isotropic state and allowed to slowly cool to the cholesteric phase. The E-O measurement was carried out by aligning the stripes of electrode of the IPS cell at a 45° angle between the 90 °Crossed polarizers. The measurements of light transmittance as a function of applied voltage curves and response times were carried out at a constant BP state at 50 °C. The BP temperature range was increased up to 3.2 °C, and decreased with increasing concentration of AuNR in the BP mixture. We observe a shift to longer wavelengths in the doped BP samples with respect to the pure BP, which is independent of the temperature; the pure BP was shifted from 485 nm to 500 nm, while 0.06% AuNR BP was shifted from 483 nm to 580 nm. This longest shift was noticed in 0.06% AuNR BP, which supports the reported POM image (Fig. 5). The electro-optical properties of the samples were investigated using IPS cells with 5/5/5 of electrode space, line width and cell gap, respectively. An applied voltage to the cells at a constant temperature of 50 °C shows the contrast between field-on (bright)

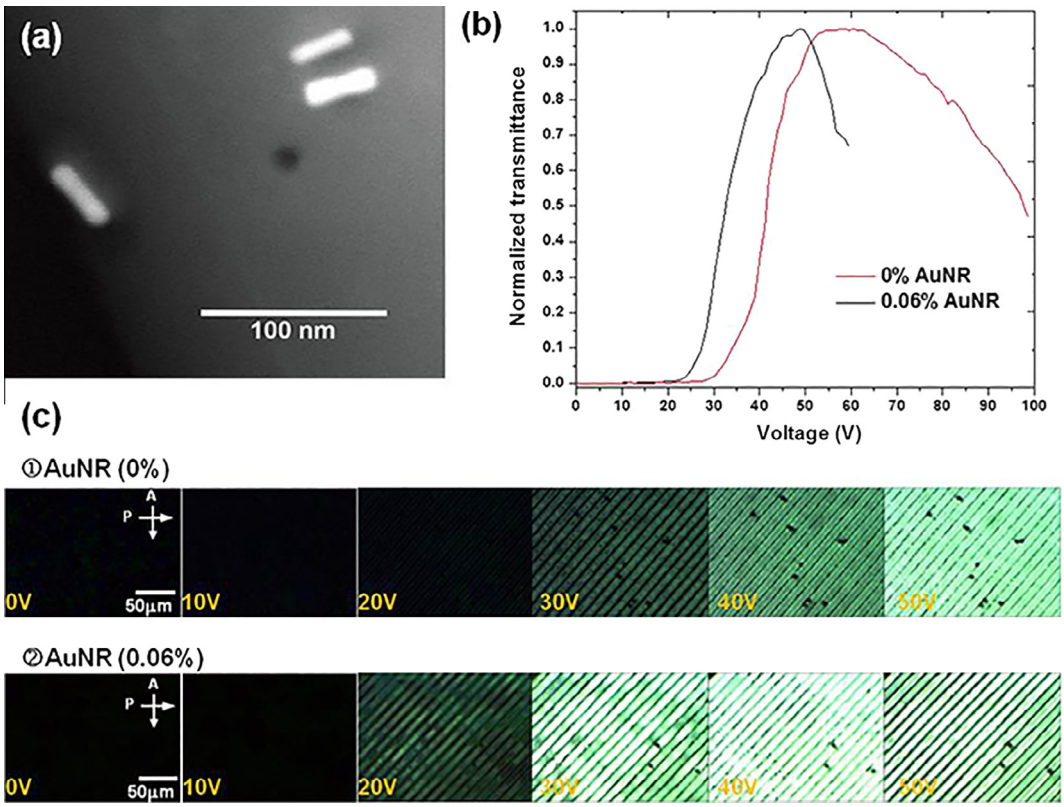

Fig. 5. (a) TEM images of organo-thio monolayer protected AuNRs in 0.0006% AuNRs in blue phase liquid crystal at 50 °C, (b) the transmittance–voltage (TV) curve of pure BP and 0.06% AuNR BP device, and (c) the POM images of (b) pure BP samples (c) 0.06% AuNR BP. The Figure is reproduced from Ref. [41]. (For interpretation of the references to colour in this figure legend, the reader is referred to the web version of this article.)

and field-off (dark) states as seen in Fig. 5b. The POM images are the manifest of the transmittance versus applied voltage curves for both pure and doped BPs (Fig. 5c). With AuNR doping the BP is switched to a stripe domain at a low voltage where the field is applied in the direction normal to the stripes. The discontinued stripes arise from imperfect electrode patterning during the substrate preparation. By contrast, the disappearance of the stripe domain for pure BP occurs at a higher voltage. The electro-optical study shows a reduction in the threshold voltage (V_{th}) of the doped 0.06% AuNR BP (V_{th} = 27.3 V) with respect to the pure BP (V_{th} = 34.6 V). The AuNRs doped BPLC exhibits the same light transmission as that of the BPLC at the field-on state at a lower voltage. One of the advantages of BPLC is its fast response time. In the measured response time of the pure BPLC, the rise time was 2.1 ms and the fall time was 1.7 ms. Conversely, in the measured response time for the 0.06% AuNR doped BPLC, the rise time was 15.3 ms and the fall time was 5.9 ms. The response time of 0.06% AuNR doped BPLC is slightly higher than that of the pure BPLC. This phenomenon can be explained by a prior report [40]. This result is because the rise time for the AuNRs doped sample would be slower if the applied voltage is close to the critical voltage to unwind the cholesteric pitches (V_c). To speed up the turn on time, one should apply an overdrive voltage to the Kerr device. The analyses of fall times imply that the fall time of AuNRs doped sample is about twice slower that of the pure BPLC. We can speculate that this could be due to the increase in rotational viscosity arising from the inclusion of AuNRs at the disclinations, which requires extra energy for local double twists to overcome the extra exclusive volume of the AuNRs [41]. In this way we have demonstrated that BP is stabilized as a result of doping AuNR. The BP temperature range was increased up to 3.2 °C, and decreased with increasing concentration of AuNR in the BP mixture. The appearance of orange and red domains in POM images is supported by reflection spectra data showing a shift to longer wavelengths with respect to non-doped BP liquid crystals. It is seen that the greatest shift in the maximum wavelength occurs with 0.06% AuNR BP. This suggests that AuNRs successfully stabilize the BP medium and optimize thermal stability at low concentrations. In the electro-optical induced Kerr effect, the optimization in the doped AuNR BP LC device also led to a reduction in threshold voltage (V_{th}); V_{th} (34.6V) of pure BP, and V_{th} (27.3V) of the doped BP mixture.

3. Polymer stabilized liquid crystals

LCs and polymers have been developed for various electro-optical applications such as light shutter, optical switch, optical lens and displays [42]. Polymer stabilized cholesteric textures (PSCTs) and polymer dispersed liquid crystals (PDLCs) technologies are widely used in these fields. For PSCTs, cholesteric textures can be stabilized by polymer network. There are three textures (states) of cholesteric liquid crystal (Ch-LC) used in PSCTs, i.e., planar (P), focal conic (FC) and homeotropic (H) states for display and photonic devices [43–46]. For normal mode PSCT, the material is optical scattering and opaque at zero fields, because the LC is in the FC state and the spatial refractive index varies between different domains in the zero fields. When an electric field is applied, the material becomes transparent since the LC is aligned in the H state by the electric field. The refractive index of the LC and the polymer are matched in this case. For reverse mode PSCT, the LC is in the P state without external fields applied due to the alignment layer on the substrate. The reflected wavelength of the P state is in the infrared range. Therefore the material is transparent at zero field. When a proper electric field is applied, the LC is changed to the

FC state. The material becomes optical scattering and opaque. The electric-optical properties of normal mode and revers mode are monostable [47], whose voltage–transmittance curved are shown in Fig. 6. We can see in the normal mode and reverse mode PSCTs, a voltage must be applied to sustain one of optical states in normal mode or reverse mode PSCTs. Later, bistable PSCT devices have been developed using positive Ch-LC [48]. The transmittance response to a voltage pulse [49] is shown in Fig. 7. Due to an energy barrier created by a certain amount of polymer or a surface aligning effect, both P state and FC state can be stable at zero field and be switched by different voltage pulses. For examples, if the initial state is FC state (scattering state), when applying a voltage pulse large than V5 (Fig. 2), the LC texture will be switched to P state (transparent state). If the initial state is P state, when applying a voltage pulse at V2, the LC texture will be change to FC state. No voltage has to be applied to sustain the optical states in the bistable PSCTs. Dual frequency LCs [50] have also been used in normal PSCT for fast response time [51] and in bistable PSCTs with P state and FC state [52]. For a dual frequency LC (DFLC), at low frequency electric field, it has a positive dielectric anisotropy and the LC molecules tend to align along the applied electric field and at high frequency electric field, the LC has a negative dielectric anisotropy and the molecules tend to align perpendicular to the applied electric field. The cross-over frequency of DFLC is the frequency where the dielectric anisotropy is zero. The low crossover frequency of dual frequency LC is favorite as it will be more suitable for practical applications. Another bistable PSCT using DFLC where the H and the FC state are stable at zero field have been developed [53], as shown in Fig. 8. The DFLC is used to switch the shutter by a low-frequency or a high-frequency electric pulse. The Ch-LC textures (H and FC state) of the material are hold at zero field by proper polymer networks. There is no power required to sustain the optical states in this system. The device is very energy-saving. Such bistable PSCT between H state and FC state is different from the conventional bistable PSCT using P state and FC state [48]. The proper polymer network, chiral dopant concentration and curing condition are the key to achieve such devices. Due to higher concentration of chiral dopant, the FC state is more scattering than conventional bistable PSCT FC mode. The contrast ratio (CR) can be 9.4:1 in a single-layered cell and further increased to 22.0:1 in a double-layered sample. This bistable light shutter can be used as architectural or greenhouse windows and electric books [54]. Afterwards, more PSCT or bistable PSCT were designed and studied [55–59]. The three states of CH-LC, H, P and FC are used to be stable by polymers or alignment layers. The LC materials (such as positive, negative or dual frequency LCs), polymers with different monomer functionalities, concentrations, curing condition (such as UV curing time, intensity and temperature), driving method including different driving voltages, frequencies or timing can be used to optimize PSCTs to get higher CR, wider viewing angle and lower driving voltage.

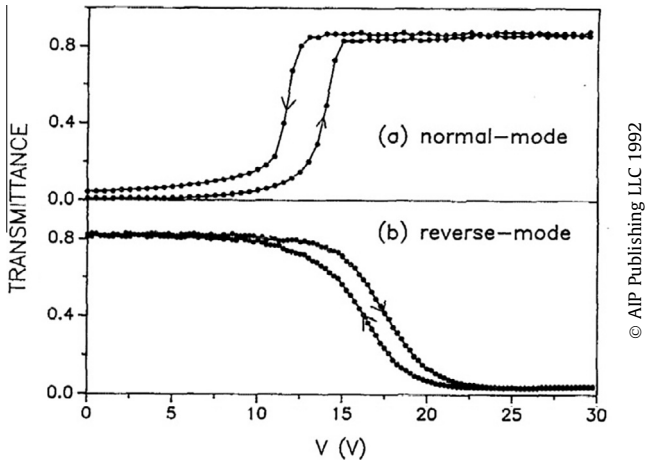

Fig. 6. Transmittance of normal mode and reverse mode of PSCT versus the applied voltage. Reprinted with permission from [47].

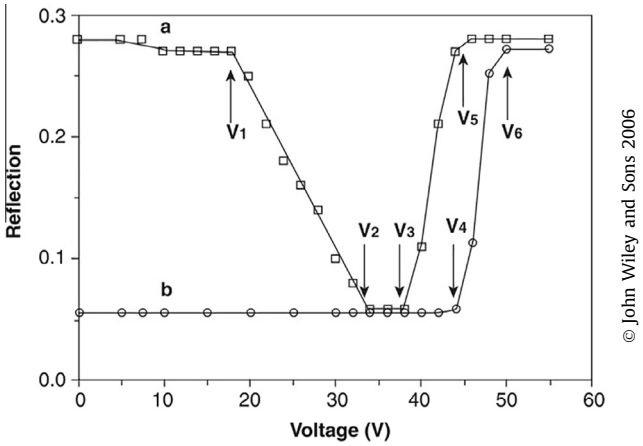

Fig. 7. Response of a bistable CH-LC to voltage pulses. (a) Initially in the planar state and (b) initially in the focal conic state. Reprinted with permission from [49].

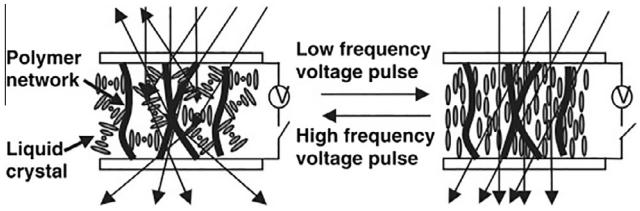

Fig. 8. Schematic diagram of a bistable PSCT light shutter using dual frequency liquid crystal.

4. Electrofluidic technology for displays

Electrowetting is often the modification of contact angle and thus hydrophobic properties of a surface by applying varying amounts of voltage. Next to LCD and OLED technology, the closest possible emerging technology that has demonstrated a considerable future potential may be electrofluidic technology. It has made its presence clear in various aspects of an ideal display product. It has been demonstrated to be useful as smart windows [60–62], sunlight steering [63] displays, video speed operable [64] displays, sunlight readable and billboard [65] displays. In addition, often these displays independently demonstrate quite a few of the established LCD specs such as color gamut, brightness [66], contrast just to name a few. The interest in this technology may well be considered to come into limelight after the work of Hayes et al. in terms of demonstrating video speed electronic paper [64]. However, often it is difficult to meet the well-established strict display standards in an integrated system that have had successfully been demonstrated by LCDs. LCDs have their limitations including strictly limited operation by the deep need to use polarizers and they are often far from a lively appeal. In other words, LCDs does not provide the picture and video quality that an unaltered printed color could provide on a printed paper. Commercializing this interesting electrowetting technology to a wide variety of customer base and consumer markets may continue to be challenging, but there are a few active and inactive spin offs that have had focused

Table 1
Physical parameters of the solution (OS30/PG).

Physical property	Measured value (±5% error)
IFT	110 dyne/cm
Surface tension (PG-pigment)	34 dyne/cm
Pigment particle size in PG (D50)	50 nm
Conductivity (PG-pigment)	4–8 μS/cm
Viscosity (PG-pigment)	62 cp

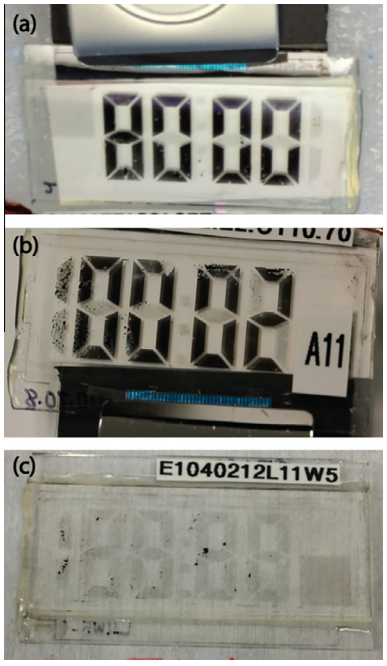

Fig. 9. Various 3.5 μm electrowetting devices in operating ON (a), (b) and OFF (c) state.

on developing various electrowetting based displays. Some of them include Varioptic, Poly Vision, Gammadynamics, and LiquaVista. Often one of the biggest issues of this technology seems to be the demanding long lifetime of the display. And such lifetime cannot be achieved without the intense research to find more immiscible polar and non-polar liquid combinations that provide clear and color states that could potentially withstand various weathering tests without compromising the display aesthetics over the lifetime of the display. In addition, the only successful company that has successfully demonstrated a fully functional and LCD comparable electrowetting may well be Samsung Netherlands R&D center [67]. Its success has been based on demonstrating electrowetting technology that is much adaptable to current liquid crystal display production lines. However, their biggest challenge and advantage may well be implementing the same for mass production of electrowetting displays and replacing expensive liquid crystal materials respectively. Over all we think, longevity of an electrowetting display is one of the key physical properties that needs more research and development. As mentioned above, such longevity is limited by the variety of available polar and non-polar fluid combinations.

Here, we focus on one of such combinations. We present results obtained by using immiscible fluid combination of propylene glycol (PG) based ink (pigment based color fluid) and OS30 (clear fluid). OS30 was used as non-polar clear fluid and PG is used as polar fluid with ~4% of black pigment dispersed in it. Interfacial tension (IFT), surface tension of PG-pigment/OS30 combination, particle size of pigment and other critical physical parameters are given in Table 1. As one may notice, IFT is function of pressure, temperature, and the composition of each phase. Transparent bottom substrate is fabricated with glass substrate and PerMX film. The film is characterized by negative working, chemically amplified dielectric epoxy polymer film made with three layer (polyester/microlithographic polymer/polyethylene layers). The film is often suitable for structuring, bonding, plating and etching applications. The bottom and corresponding top substrate are coated with 600 nm/100 nm layers of Parylene-C/Cytop layers respectively. The cell gap of the electrowetting devices is controlled at 3.5 μm. The device is filled and assembled using above mentioned low-ion pigment based PG/OS30 (polar/non-polar) fluid combination. The cell gap was well controlled and observed more than ~95% fill factor. Fig. 9a and b shows various electrowetting devices in ON-state and Fig. 9c shows the device in OFF state. However, it is often challenging to provide a quality device that demonstrate long life operation of more than ~100 h with no variation in the image quality. Figs. 10a, b and 11a, b show contrast variation at 0, 1, 5 and 30 h operation respectively on a different operating segment of the device with a larger cell gap. And Fig. 11c shows contrast variation after 25 h continuous operation from 5 h to 30 h or it is the contrast difference between 5 h and 25 h operated device. In 3 days of operation, fewer than <50% pixels showed either full actuation or retained initial contrast. Only a

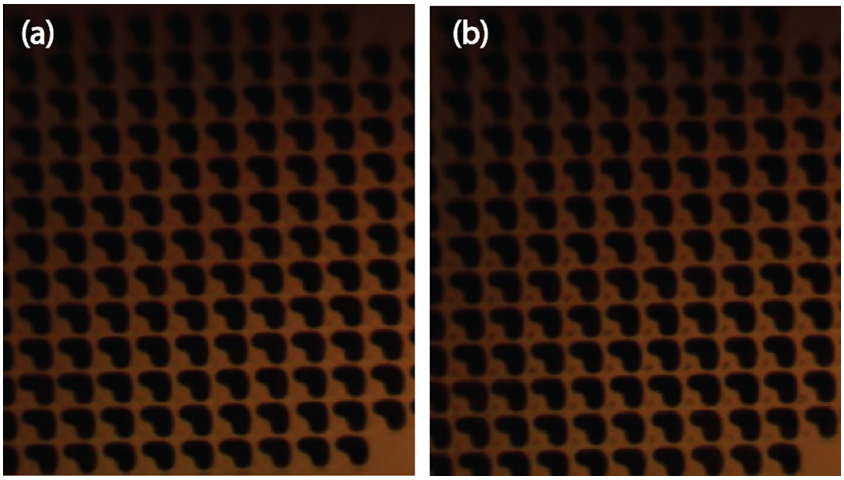

Fig. 10. Low ion ink filled electrowetting device in the ON state after 0:00 h (a) and 1:00 h (b).

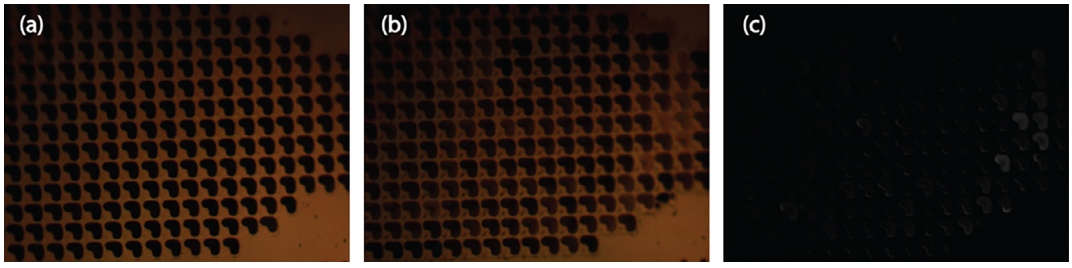

Fig. 11. Electrowetting device in the ON state after 5:00 h (a) and 30:00 h (b). (c) Represents the contrast variation obtained after 25 h.

few than 25% of pixels showed both characteristics. Possible important reasons for varying pixel-to-pixel contrast variation in 20–30 h is unexpected and is not clearly understand. The main reasons for short lifetime of this combination of materials may not be non-polar fluid, PerMX layer, ITO and drive electronics. The main issue may potentially be the quality of dielectric layer, which is Parylene-C, and possible breakdown of color pigment in the polar fluid. There may be impurities as well in the pigment that might be causing ink breakdown. Small particle break down in the pigment may cause large particles in the ink and they also may cause varying degrees of phase (fast/slow) separation thus leading to contrast changes. The quality of ITO has not been checked on the bottom and top substrates before and after device operation, but the varying possible impurities from Paralyne C may expose PG to varying ITO lines/areas to change effective voltage experienced by the pixels. The critical next steps may need to be understanding chemistry of polymer/PG/pigment diffusion into the non-polar fluid OS30. Or in a broader way understand the diffusion mechanism between polar and non-polar fluids under varying circumstances of temperature and intense and prolonged device operation.

5. Conclusion

We have reported an overview of recent advances in LCD applications. Particularly, in order to eliminate the need for any mechanical alignment and rubbing process for future LCD panel development, we have proposed a "surfactant free" method based on periodic structures realized through nanoimprint lithography, interference holography and polymer stabilized LCs. Further, we have reported on the possibility to improve the optical and electro-optical properties of modern LCD by combing the properties of LCs blue phase and nanomaterials. In particular, we have observed that the response time can be improved by doping a cholesteric liquid crystal blue phase with gold nanorods. Finally, we have analyzed an emerging technology for further improve novel displays based on the modification of the wetting properties of a surface. Electrowetting technology has the capability to realize high quality images that ensure excellent indoor and outdoor readability while minimizing the battery consumption.

Acknowledgments

E.S.P. Leong and Y.J. Liu thank the funding support from Joint Council Office (JCO) of the Agency for Science, Technology and Research (A*STAR) under the Grant No. 12302FG012. G. Palermo and L. De Sio thank the funding support from the Air Force Office of Scientific Research (AFOSR), Air Force Research Laboratory (AFRL), U.S. Air Force, under Grant FA9550-14-1-0050 (P.I. L. De Sio, EOARD 2014/2015) and the Materials and Manufacturing Directorate, AFRL.

References

[1] P. Slikkerveer, P. Bouten, P. Cirkel, J. de Goede, H. Jagt, N. Kooyman, G. Nisato, R. van Rijswijk, P. Duineveld, A fully flexible colour display, SID Symp. Dig. Tech. Pap. 35 (2004) 770–773.
[2] S. Varghese, S. Narayanankutty, C.W.M. Bastiaansen, G.P. Crawford, D.J. Broer, Patterned alignment of liquid crystals by μ-rubbing, Adv. Mater. 16 (2004) 1600–1605.
[3] J. Osterman, C. Ad_as, L. Madsen, K. Skarp, Properties of azo-dye alignment layer on plastic substrates, SID Symp. Dig. Tech. Pap. 36 (2005) 772–775.
[4] V. Konovalov, V. Chigrinov, H.S. Kwok, H. Takada, H. Takatsu, Photoaligned vertical aligned nematic mode in liquid crystals, Japan J. Appl. Phys. 43 (2004) 261–266.
[5] W. Gibbons, P. Shannon, S.T. Sun, B. Swetlin, Surface-mediated alignment of nematic liquid crystals with polarized laser light, Nature 351 (1991) 49–50.
[6] D. Andrienko, Y. Kurioz, Y. Reznikov, C. Rosenblatt, R. Petschek, O. Lavrentovich, D. Subacius, Tilted photo-alignment of a nematic liquid crystal induced by a magnetic field, J. Appl. Phys. 83 (1998) 50–55.
[7] J.K. Kim, C.J. Choi, J.S. Park, S.J. Jo, B.H. Hwang, M.K. Jo, D. Kang, S.J. Lee, Y.S. Kim, H.K. Baik, Orientational transition of liquid crystal molecules by a photoinduced transformation process into a recovery free silicon oxide layer, Adv. Mater. 20 (2008) 3073–3078.
[8] P. Chaudhari, J. Lacey, S.A. Lien, J. Speidell, Atomic beam alignment of liquid crystal, Japan J. Appl. Phys. 37 (1998) L55–L56.
[9] P. Chaudhari, J. Lacey, J. Doyle, E. Galligan, S.-C.A. Lien, A. Callegari, G. Hougham, N.D. Lang, P.S. Andry, R. John, K.-H. Yang, M. Lu, C. Cai, J. Speidell, S. Purushothaman, J. Ritsko, M. Samant, J. Stöhr, Y. Nakagawa, Y. Katoh, Y. Saitoh, K. Sakai, H. Satoh, S. Odahara, H. Nakano, J. Nakagaki, Y. Shiota, Atomic-beam alignment of inorganic materials for liquid crystal displays, Nature 411 (2001) 56–59.
[10] L. Janning, Thin film surface orientation for liquid crystal, Appl. Phys. Lett. 21 (1972) 173.
[11] K.C. Kim, H.J. Ahn, J.B. Kim, B.H. Hwang, H.K. Baik, Novel alignment mechanism of liquid crystal on a hydrogenated amorphous silicon oxide, Langmuir 21 (2005) 11079–11084.
[12] D.W. Berreman, Solid surface shape and the alignment of an adjacent nematic liquid crystal, Phys. Rev. Lett. 28 (1972) 1683–1684.
[13] D.W. Berreman, Alignment of liquid crystals by grooved surfaces, Mol. Cryst. Liq. Cryst. 23 (1973) 215–231.
[14] Y.J. Liu, W.W. Loh, E.S.P. Leong, T.S. Kustandi, X.W. Sun, J.H. Teng, Nanoimprinted ultrafine line and space nanogratings for liquid crystal alignment, Nanotechnology 23 (2012) 465302–465307.
[15] S.Y. Chou, P.R. Krauss, P.J. Renstrom, Nanoimprint lithography, J. Vac. Sci. Technol., B 14 (1996) 4129–4133.
[16] M.D. Austin, H. Ge, W. Wu, M. Li, Z. Yu, D. Wasserman, S.A. Lyon, S.Y. Chou, Fabrication of 5 nm linewidth and 14 nm pitch features by nanoimprint lithography, Appl. Phys. Lett. 84 (2004) 5299–5301.
[17] L.J. Guo, Nanoimprint lithography: methods and material requirements, Adv. Mater. 19 (2007) 495–513.
[18] S.Y. Yew, T.S. Kustandi, H.Y. Low, J.H. Teng, Y.J. Liu, E.S.P. Leong, Single-material-based multilayered nanostructures fabrication via reverse thermal nanoimprinting, Microelectron. Eng. 88 (2011) 2946–2950.
[19] E.S.P. Leong, S.Y. Yew, T.S. Kustandi, Y.J. Liu, H. Tanoto, Q.Y. Wu, W.W. Loh, S.L. Teo, J.H. Teng, New approach for multilayered microstructures fabrication based on a water-soluble backing substrate, ACS Appl. Mater. Interfaces 5 (2013) 5898–5902.
[20] E.S.P. Leong, S.J. Wu, N. Zhang, W.W. Loh, E.H. Khoo, G.Y. Si, H.T. Dai, Y.J. Liu, Optical properties of ultrafine line and space polymeric nanogratings coated with metal and metal-dielectric-metal thin films, Nanotechnology 25 (2014) 055203–055208.
[21] H.-R. Kim, J.-W. Jung, Y.-J. Lee, J.-H. Kim, Liquid crystal alignment with a molecular template of imprinted polymer layer during phase separation, Appl. Phys. Lett. 88 (2006). 113504-3.
[22] J.S. Gwag, M. Oh-e, M. Yoneya, H. Yokoyama, H. Satou, S. Itami, Advanced nanoimprint lithography using a graded functional imprinting material tailored for liquid crystal alignment, J. Appl. Phys. 102 (2007). 063501-3.
[23] Y. Yi, M. Nakata, A.R. Martin, N.A. Clark, Alignment of liquid crystals by topographically patterned polymer films prepared by nanoimprint lithography, Appl. Phys. Lett. 90 (2007). 163510-3.

[24] R.S. Lin, J.A. Rogers, Molecular-scale soft imprint lithography for alignment layers in liquid crystal devices, Nano Lett. 7 (2007) 1613–1621.
[25] H.-G. Park, J.-J. Lee, K.-Y. Dong, B.-Y. Oh, Y.-H. Kim, H.-Y. Jeong, B.-K. Ju, D.-S. Seo, Homeotropic alignment of liquid crystals on a nano-patterned polyimide surface using nanoimprint lithography, Soft Matter 7 (2011) 5610–5614.
[26] H. Takahashi, T. Sakamoto, H. Okada, Liquid crystal device with 50 nm nanogroove structure fabricated by nanoimprint lithography, J. Appl. Phys. 108 (2010). 113529-3.
[27] N. Ishizawa, K. Idei, T. Kimura, D. Noda, T. Hattori, Resin micromachining by roller hot embossing, Microsyst. Technol. 14 (2008) 1381–1388.
[28] C.J. Ting, F.Y. Chang, C.F. Chen, C.P. Chou, Fabrication of an antireflective polymer optical film with subwavelength structures using a roll-to-roll micro-replication process, J. Micromech. Microeng. 18 (2008). 075001-6.
[29] S.H. Ahn, L.J. Guo, Large-area roll-to-roll and roll-to-plate nanoimprint lithography: a step toward high-throughput application of continuous nanoimprinting, ACS Nano 3 (2009) 2304–2310.
[30] R. Caputo, L. De Sio, A. Veltri, C. Umeton, A.V. Sukhov, Development of a new kind of switchable holographic grating made of liquid-crystal films separated by slices of polymeric material, Opt. Lett. 29 (2004) 1261–1263.
[31] L. De Sio, A. Veltri, A. Tedesco, R. Caputo, C. Umeton, A.V. Sukhov, Characterization of an active control system for holographic setup stabilization, Appl. Opt. 47 (2008) 1363–1367.
[32] L. De Sio, S. Serak, N. Tabiryan, C. Umeton, Mesogenic versus non-mesogenic azo dye confined in a soft-matter template for realization of optically switchable diffraction gratings, J. Mater. Chem. 21 (2011) 6811–6814.
[33] L. De Sio, S. Ferjani, G. Strangi, C. Umeton, R. Bartolino, Soft periodic microstructures containing liquid crystals, J. Phys. Chem. B 117 (2013) 1176–1185.
[34] L. De Sio, S. Ferjani, G. Strangi, C. Umeton, R. Bartolino, Universal soft matter template for photonic applications, Soft Matter 7 (2011) 3739–3743.
[35] L. De Sio, P. D'Aquila, E. Brunelli, G. Strangi, D. Bellizzi, G. Passarino, C.P. Umeton, R. Bartolino, Directed organization of DNA filaments in a soft matter template, Langmuir 29 (2013) 3398–3403.
[36] L. De Sio, N. Tabiryan, T. Bunning, Spontaneous radial liquid crystals alignment on curved polymeric surfaces, Appl. Phys. Lett. 104 (2014). 221112-4.
[37] D.C. Wright, N.D. Mermin, Crystalline liquids: the blue phases, Rev. Mod. Phys. 61 (1989) 385–432.
[38] H. Kikuchi, M. Yokota, Y. Hisakado, H. Yang, T. Kajiyama, Polymer-stabilized liquid crystal blue phases, Nat. Mater. 1 (2002) 64–68.
[39] J. Yan, S.T. Wu, Polymer-stabilized blue phase liquid crystals: a tutorial, Opt. Mater. Exp. 1 (2011) 1527–1535.
[40] H. Choi, H. Higuchi, H. Kikuchi, Electro-optic response of liquid crystalline blue phases with different chiral pitches, Soft Matter 7 (2011) 4252–4256.
[41] J.-M. Wong, J.-Y. Hwang, L.-C. Chien, Electrically reconfigurable and thermally sensitive optical properties of gold nanorods dispersed liquid crystal blue phase, Soft Matter 7 (2011) 7956–7959.
[42] S.-T. Wu, D.-K. Yang, Reflective Liquid Crystal Displays, John Wiley & Sons Inc., New York, 2001.
[43] H. Ren, S.-T. Wu, Reflective reversed-mode polymer stabilized cholesteric texture light switches, J. Appl. Phys. 92 (2002) 797–800.
[44] J. Ma, L. Xuan, Towards nanoscale molecular switch-based liquid crystal displays, Displays 34 (2013) 293–300.
[45] W.-L. Hsu, J. Ma, M. Graham, K. Balakrishnan, S. pau, Patterned cholesteric liquid crystal polymer film, J. Opt. Soc. Am. A 30 (2013) 252–258.
[46] R. Wu, Y. Li, J. Wu, J. Ma, Q. Dai, A study of lasing wavelength by DOS in the temperature-tunable cholesteric liquid crystal lasers, Opt. Commun. 300 (2013) 1–4.
[47] D.-K. Yang, L.-C. Chien, J.W. Doane, Cholesteric liquid crystal/polymer dispersion for haze free light shutters, Appl. Phys. Lett. 60 (1992) 3102–3104.
[48] D.-K. Yang, X.-Y. Huang, Y.-M. Zhu, Bistable cholesteric reflective displays: materials and drive schemes, Annu. Rev. Mater. Sci. 27 (1997) 117–146.
[49] D.-K. Yang, S.-T. Wu, Fundamentals of Liquid Crystal Devices, John Wiley & Sons Inc., New York, 2006.
[50] H. Xianyu, S.-T. Wu, C.-L. Lin, Dual frequency liquid crystals: a review, Liq. Cryst. 36 (2009) 717–726.
[51] M. Xu, D.-K. Yang, Dual frequency cholesteric light shutters, Appl. Phys. Lett. 70 (1997) 720–722.
[52] M. Xu, D.-K. Yang, Electrooptical properties of dual-frequency cholesteric liquid crystal reflective display and drive scheme, Jpn. J. Appl. Phys. 38 (1999) 6827–6830.
[53] J. Ma, L. Shi, D.-K. Yang, Bistable polymer stabilized cholesteric texture light shutter, Appl. Phys. Exp. 3 (2010) 021702.
[54] D.K. Yang, Review of operating principle and performance of polarizer-free reflective liquid-crystal displays, J. SID 16 (2008) 117–124.
[55] Y.-C. Hsiao, C.-Y. Tang, W. Lee, Fast-switching bistable cholesteric intensity modulator, Opt. Express 19 (2011) 9744–9749.
[56] H.-H. Liang, C.-C. Wu, P.-H. Wang, J.-Y. Lee, Electro-thermal switchable bistable reverse mode polymer stabilized cholesteric texture light shutter, Opt. Mater. 33 (2011) 1195–1202.
[57] Y.-C. Hsiao, C.-T. Hou, V.Y. Zyryanov, W. Lee, Multichannel photonic devices based on tristable polymer-stabilized cholesteric textures, Opt. Express 19 (2011) 23952–23957.
[58] P. Kumar, S.-W. Kang, S.H. Lee, Advanced bistable cholesteric light shutter with dual frequency nematic liquid crystal, Opt. Mater. Exp. 2 (2012) 1121–1134.
[59] K.-H. Kim, B.-H. Yu, S.-W. Choi, S.-W. Oh, T.-H. Yoon, Dual mode switching of cholesteric liquid crystal device with three-terminal electrode structure, Opt. Express 20 (2012) 24376–24381.
[60] H. You, A.J. Steckl, Versatile electrowetting arrays for smart window applications-from small to large pixels on fixed and flexible substrates, Sol. Energy. Mat. Sol. Cells 117 (2013) 544–548.
[61] S.W. Kuo, K.L. Lo, W.Y. Cheng, H.H. Lee, Y.H. Tsai, Y.S. Ku, P.P. Cheng, P.-J. Su, J.W. Shiu, A novel electrowetting-based display for future smart window application, SID Symp. Dig. Tech. Pap. 42 (2011) 232–235.
[62] Unpublished Gammadynamics R&D Work by Hari Atkuri/Ken Dean/Jason Heikenfeld.
[63] J. Cheng, S. Park, C.L. Chen, Optofluidic solar concentrators using electrowetting tracking: concept, design, and characterization, Sol. Energy 89 (2013) 152–161.
[64] R.A. Hayes, B.J. Feenstra, Video-speed electronic paper based on electrowetting, Nature 425 (2003) 383–385.
[65] K. Blankenbach, M. Jentsch, J. Rawert, D. Jerosch, A. Bitman, F. Bartels, Sunlight readable bistable electrowetting displays for indicators and billboards, SID Symp. Dig. Tech. Pap. 42 (2011) 1527–1530.
[66] J. Heikenfeld, M. Hagedon, A. Russell, S. Yang, E. Kreit, K. Zhou, S. Smith, H. Atkuri, L. Salem, K. Dean, J. Rudolph, A high-brightness electrofluidic display film, SID Symp. Dig. Tech. Pap. 43 (2012) 75–78.
[67] http://www.samsung.com/global/business/semiconductor/aboutus/business/openinnovation/operation-overseas-research-centers.